Contents lists available at ScienceDirect

Chemosphere

Supported Pd/Sn bimetallic nanoparticles for reductive dechlorination of aqueous trichloroethylene

Chin Jung Lin [a], Ya Hsuan Liou [b], Shang-Lien Lo [a,*]

[a] Research Center for Environmental Pollution Prevention and Control Technology, Graduate Institute of Environmental Engineering,
National Taiwan University, 71, Chou-Shan Road, Taipei 106, Taiwan, ROC
[b] Department of Geosciences, National Taiwan University, P.O. Box 13-318, Taipei 106, Taiwan, ROC

ARTICLE INFO

ABSTRACT

A Pd/Sn bimetallic nanoparticles resin (nano-Pd/Sn/resin) was successfully synthesized for reductive transformation of aqueous trichloroethylene (TCE). The physicochemical properties of the prepared resin were characterized using scanning electron microscopy, energy dispersive X-ray spectroscopy, N_2 isothermal sorption at and X-ray photospectroscopy. The surface-area-normalized rate constants (k_{SA}) of Sn particles in the nanoscale range (50–100 nm) were 4.5 times larger than the k_{SA} for powdered Sn (0.04 mm). After depositing 1 wt% Pd onto nano-Sn surface, k_{SA} was further enhanced by about a factor of 2. Groundwater constituents such as sulfide nitrate and dissolved oxygen had significant negative effects on the rate of TCE degradation by the nano-Pd/Sn/resin. A wet-chemical method regeneration method was observed to effectively restore the reactivity of the poisoned nano-Pd/Sn/resin after dipping in sulfide solution for 2 d. In all cases, less than 0.5% of the degraded TCE appeared as chlorinated byproducts including the three dichloroethene isomers. The nano-Pd/Sn/resin technique performs well in transforming TCE into nontoxic hydrocarbons, as compared with other published methods.

1. Introduction

Destroying aqueous chlorinated organics for environmental remediation requires either high-energy processes (Qin et al., 2001) or complex equipment (Drijvers et al., 1999; Yamazaki et al., 2001), effectively restricting field scale application. Biological processes may be effective, but conditions must be well controlled to enable microorganisms to grow. Conventional physicochemical methods accompanying the use of expensive chemicals or high energies largely restrict application at the field scale. Thus, they may not always be practical. Phytoremediation, using the ability of plants to remove and degrade chlorinated solvents, may offer a cost-effective, in situ, and safe alternative to conventional physicochemical methods (McCutcheon and Schnoor, 2003). Since Gillham and co-workers (Renolds et al., 1990; Gillham and O'Hannesin, 1994) proposed the transformation of halogenated aliphatic compounds in the presence of zero-valent iron (ZVI), the use of ZVI as a reductant has been considered as a promising alternative to conventional physicochemical methods. Recently however, several drawbacks associated with the reaction between ZVI and chlorinated organics have been reported, including: (1) possible metal oxide precipitation at elevated pH (Chen et al., 2001; Su and Puls, 2004); (2) accumulation of toxic chlorinated by-products

associated with a decrease in ZVI reactivity over time (Su and Puls, 1999; Cheng and Wu, 2000; Doong et al., 2003); and the (3) the frequent and costly replacement of exhausted ZVI powder.

Improved methods for rapid and complete dechlorination include: (1) alternative metals, such as Zn, Mg, Sn and Si (Boronina and Klabunde 1995; Doong et al., 2003); (2) combining ultrasound (Hung and Hoffmann, 1998) with ZVI; (3) exploiting the synergistic effect of cationic surfactants and ZVI (Alessi and Li, 2001); (4) reducing particle size into the nanoscale range (Wang and Zhang, 1997; Choe et al., 2000; Feng and Lim, 2005) and (5) deposition of a second reactive metal, such as Ni, Cu, Pt, Pd and Au (Muftikian et al., 1995; Grittini et al., 1995; Kim and Carraway, 2000; Lin et al., 2004; Liou et al., 2005). Among these, depositing the second metal onto ZVI nanoparticles is the most promising due to dramatically enhanced reactivity and nontoxic product selectivity. The benefit of bimetallic nanoparticles, however, is short-lived due to the formation of metal oxide and hydroxide films, chemisorption of compounds on active sites or loss of loosely bound secondary metal particles. The regeneration of bimetal activity by treatment with reducing agents has been demonstrated (Lowry and Reinhard, 2000), but an efficient method to restore the reactivity of bimetals for field applications is still lacking.

Several studies have reported that attachment of metallic particles onto polymer membranes and zeolite to avoid problems, such as the reduction of particle loss, prevention of particles agglomeration, and potential application of convective flow, which occurred

* Corresponding author. Tel.: +886 223625373; fax: +886 223928830.
E-mail address: sllo@ntu.edu.tw (S.L. Lo).

by freestanding ZVI (Li et al., 1999; Meyer et al., 2004; Xu et al., 2005; Li et al., 2007). Several advantages associated with the reduction of chlorinated organic compounds by zero-valent metal supported on a resin are as follows: (1) as the reaction proceeds, H$^+$ or Na$^+$ ions are released from the acidic cation resin to exchange equivalent metal ions and cause acidic conditions, which can inhibit precipitation of metal salts. (2) Adsorption of chlorinated organic compounds by this polymer matrix decreases the risk associated with the passing of chlorinated organic compounds through the treatment system. (3) The design of lightweight and flexible reductive composite material would facilitate the development of a process with convenient emplacement and regeneration. The resin-based approach requires a low-temperature process to transfer metal ions into zero-valent metal because the resin only withstands process temperatures below 300 °C. Thus, only metals with low reductive potential, e.g. Cu, have been reported for dechlorinating specific chlorinated organic compounds, such as CCl$_4$.

Tin has been demonstrated to effective remediate water containing chlorinated hydrocarbons (Boronina and Klabunde, 1995), and exhibits relative stability to ZVI in groundwater. Based on these reasons, Sn was chosen as an electron donor to degrade trichloroethylene (TCE) and noble metal, Pd, was used to promote its reactivity to dechlorination reaction. We describe a straightforward preparation method to support nano-Pd/Sn bimetals on a cation resin using wet-chemical processes under ambient conditions. The properties of the resulting materials were characterized by scanning electron microscopy (SEM), energy dispersive X-ray spectroscopy (EDX), N$_2$ isothermal sorption at 77 K and X-ray photospectroscopy (XPS). Our objectives were to evaluate: (1) the dechlorination rate; (2) the solute effects and (3) the reductive nano-Pd/Sn/resin regeneration.

2. Materials and methods

2.1. Chemicals

High-pressure liquid chromatography grade TCE, cis-dichloroethylene (cis-DCE), trans-dichloroethylene (trans-DCE) and 1,1-dichloroethylene (1,1-DCE) were obtained from Aldrich chemical (USA). Tin nitrate trihydrate was obtained from Alfa Aesar (USA), and tin powder was obtained from Riedel-de Haen (approx. 0.04 mm, >99.5%, GR grade, USA). The NaCl, NaHS, SnCl$_2 \cdot$ 2H$_2$O, PdCl$_2 \cdot n$H$_2$O (n = 3–5) and NaBH$_4$ were obtained from Aldrich Chemical. N-[2-Hydroxyethyl]piperazine-N-[2-ethanesulfonic acid] acid (HEPES, Sigma) was used for pH control. All other chemicals used in this work were analytical reagent grade, and solutions were prepared in water purified with a Milli-QTM system (18.2 MΩ cm).

2.2. Preparation of nano-Pd/Sn/resin

The resin was first loaded with the desired concentration of Sn^{2+} via ion exchange, followed by thorough washing to remove excess physisorbed Sn^{2+} ions. After washing, a 10 wt% sodium borohydride (NaBH$_4$) solution was carefully added to cause the reduction of Sn^{2+} to Sn^0, obtaining the reductant nano-Sn/resin. Electrons from the reducing agent (NaBH$_4$) were transferred to Sn^{2+} according to the following equation:

$$Sn^{2+}-(resin)^{2-} + 2NaBH_4 + 6H_2O$$
$$\rightarrow Sn^0/2Na^+-(resin)^{2-} + 2B(OH)_3 + 7H_2 \quad (1)$$
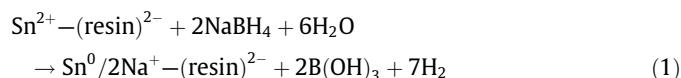
The reaction above was carried out at ambient temperature with magnetic stirring. Subsequently, the as-prepared nano-Sn/resin was poured into the acidic solution of Pd precursor with magnetic stirring, similar to our previous study (Lin et al., 2004; Liou et al.,

2007). The deposition of Pd onto the surface of Sn^0 occurred through the following redox reaction:

$$Sn^0 + Pd^{4+} \rightarrow Sn^{4+} + Pd^0 \quad (2)$$

The resulted nano-Pd/Sn/resin was then washed twice with Milli-Q water, followed by filtering and freeze-dried (27 kPa at −56 °C for 24 h).

2.3. Characterization of nano-Pd/Sn/resin

The morphology of the resulting nano-Pd/Sn/resin was viewed with SEM (Hitachi S-900) and localized elemental information from the chosen region with EDX in conjunction with SEM. The surface area measurements were performed using a N$_2$ adsorption isotherm at 77 K (Micrometer, ASAP2010). The XPS measurements were performed with a Vacuum Generators Ltd. ECSALAB MKΠ photoelectron spectrometer (East Grinstead, UK) with an Al Kα1,2 (1486.6 eV) X-ray source and a hemispherical 150 mm mean radius electron analyzer. The binding energies of the photoelectrons were determined with the assumption that the carbon 1s electrons were at 284.5 eV. During the data acquisition, the pressure in the sample chamber did not exceed 6.7×10^{-8} Pa. The weight ratio of Pd and Sn on a resin was analyzed using inductively coupled plasma atomic emission spectroscopy (ICP-AES, Varian) after the nano-Pd/Sn/resin completely dissolved in the autoclave containing a solution of HF and HNO$_3$ with a ratio of 1/4 (v/v) at 150 °C.

2.4. Batch experiments

All dynamic experiments for the degradation of TCE by nano-Pd/Sn/resin were performed in a closed batch system with zero headspace (pH 7.1–7.3). In these systems, 0.4 g of nano-Pd/Sn/resin was added into a 15 mL amber serum vial, sequentially filled with Ar-purged unbuffered Milli-QTM water. The vials were immediately capped with Teflon silicone septa and aluminum seals. A 100 μL aliquot of TCE (1100 mg L^{-1}) was then added through the septa and mixed in darkness on a rotary shaker (50 rpm) at room temperature (25 °C). Gaseous TCE and chlorinated intermediates were measured using a HP5890 GC equipped with a DB-624 capillary column and an electron capture detector operated in the splitless mode. Temperature conditions were programmed as follows: oven temperature at 50 °C; injection port temperature at 280 °C; detector temperature at 300 °C. Ultrapure nitrogen was used as carrier gas for GC at a flow rate of 4.16 mL min^{-1}. Peaks were quantified by comparing retention time and peak areas with standard gas (Supelco). All measurements were done with triplicate experiments, which indicated that the coefficient of variation was below 5%. The concentration of chloride ions in the solution was detected using an ion chromatograph (Dionex DX-100). The pH was measured with a Beckman Model 71 pH meter.

A separate experiment in a closed batch system with headspace of 2 mL were performed to analyze hydrocarbon products using a Hewlett–Packard Model 5790A GC equipped with a flame ionization detector and a GS-Q capillary column. The carrier gas was helium with 5 mL min^{-1}, and the column temperature was held at 80 °C. Fifty microliters of headspace samples were injected using a syringe. The gaseous products were identified using this method as only ethylene.

3. Results and discussion

3.1. Characterization of nano-Pd/Sn/resin

The prepared nano-Pd/Sn/resin was viewed using SEM/EDX with a magnification of 80 000, accompanied by EDX mappings of

Sn and Pd elements (Fig. 1). The size of bimetallic nanoparticle ranged between 50 and 100 nm. EDX mapping showed that Sn and Pd elements were located near each other on the surface of the resin. As shown in Fig. 2, the Sn2p3/2 and Pd3d5/2 peaks at binding energies of 487.9 and 335.1 eV found in the XPS spectra of the resin indicate that nearly all of the tin and palladium on the resin surface were present as Sn^0 and Pd^0 (Moulder et al., 1995). The specific surface areas measured using N_2 adsorption at 77 K by BET analysis were 0.004, 0.168, 0.104 and 0.112 $m^2\,g^{-1}$ for resin, powdered Sn, Sn^0 resin and nano-Pd/Sn/resin, respectively. The loadings of Pd and Sn on the resin were 0.1 $mg\,g^{-1}$ resin and 11 $mg\,g^{-1}$ resin, respectively, corresponding to a ratio of 1/110 (w/w). Considering the BET surface area of the resin and the loading amount of spherical Sn and Pd/Sn nanoparticles, the BET surface areas of the Sn and Pd/Sn nanoparticles were ∼9 $m^2\,g^{-1}$, corresponding to ∼90 nm in diameter (back-calculation from BET surface areas by assuming

Fig. 2. X-ray photospectroscopy of Sn 2p and Pd 3d on nano-Pd/Sn/resin.

that particles are spherical, and the contact between the spherical nano-Sn particle and the resin is neglected).

3.2. Degradation of TCE

The following proposed reaction pathways have been reported for the reductive degradation of TCE via zero-valent metals (Roberts et al., 1996): (1) β-elimination, which forms chloroacetylene and then rapidly transforms to completely dechlorinated products such as acetylene, ethylene and ethane; (2) hydrogenolysis that produces DCE isomers including *trans*-DCE, *cis*-DCE and 1,1-DCE; (3) hydrogenation, that produces chloroacetylene. In this study, only dichloroethylene isomers (*trans*-DCE, *cis*-DCE and 1,1-DCE) and ethylene were detectable chlorinated byproducts and end product as the reaction proceeded. Thus, the two parallel reactions, β-elimination and hydrogenolysis, with reduction of TCE and release of chloride ions were considered as a pseudo-first-order model as follows:

$$\beta\text{-elimination reaction}: \quad TCE \xrightarrow{K_1} \text{hydrocarbons} + 3Cl^- \qquad (3)$$

$$\text{hydrogenolysis reaction}: \quad TCE \xrightarrow{K_2} \text{DCE-isomers} + Cl^- \qquad (4)$$

$$[TCE] = [TCE]_0 e^{-k_{obs}t} \qquad (5)$$

$$k_{obs} = k_1 + k_2 \qquad (6)$$

where k_{obs} is the overall pseudo-first-order reaction rate constant for TCE disappearance in h^{-1}, t is reaction time in h and k_1 and k_2
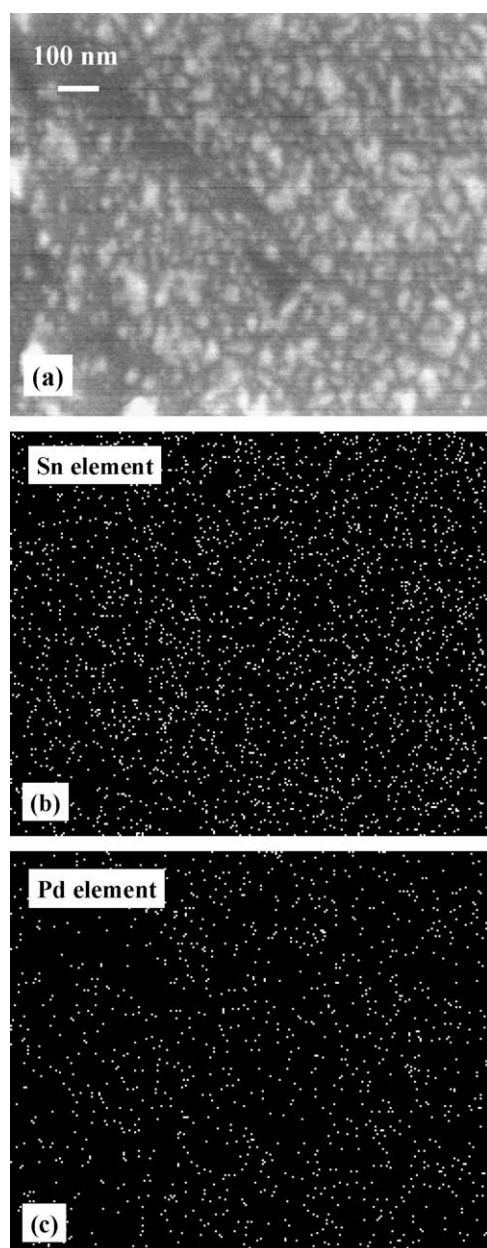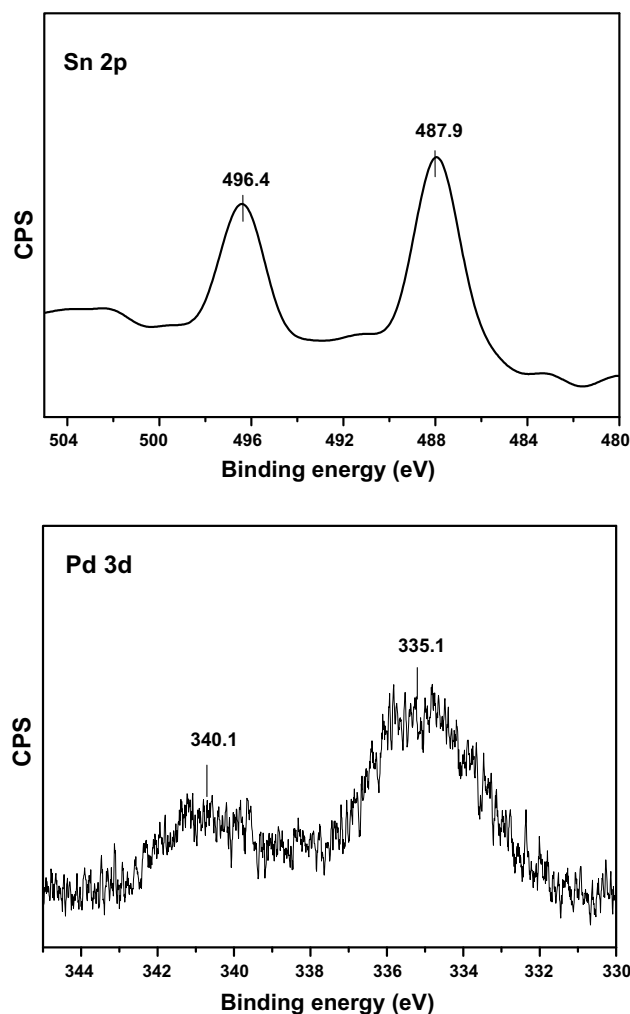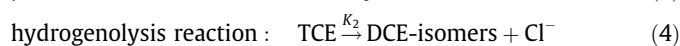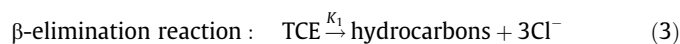
Fig. 1. Scanning electron microscopy/energy dispersive X-ray spectroscopy of nano-Pd/Sn/resin.

are the rate constants for the formation of hydrocarbons and the DCE isomers in h^{-1}, respectively. The carbon and chloride mass balance are expressed in Eqs. (7) and (8)

Carbon mass balance:

$$[TCE]_0 = [TCE]_t + [DCE\text{-}isomers]_t + [hydrocarbons]_t \qquad (7)$$

Chloride mass balance:

$$[Excess\text{-}free\text{-}Cl^-]_t = [Total\ measured\text{-}Cl^-]_t - [Cl^-(DCEs)]_t \qquad (8)$$

where $[Excess\text{-}free\text{-}Cl^-]_t$ refers to the mol of chloride ions come from the dechlorination reaction by β-elimination (Eq. (3)), [Total measured-$Cl^-]_t$ is the measured mol of chloride ions by the ion chromatograph, and $[Cl^-\text{-}(DCEs)]t$ is the mol of chloride ions come from the dechlorination reaction by hydrogenolysis (Eq. (4)). The

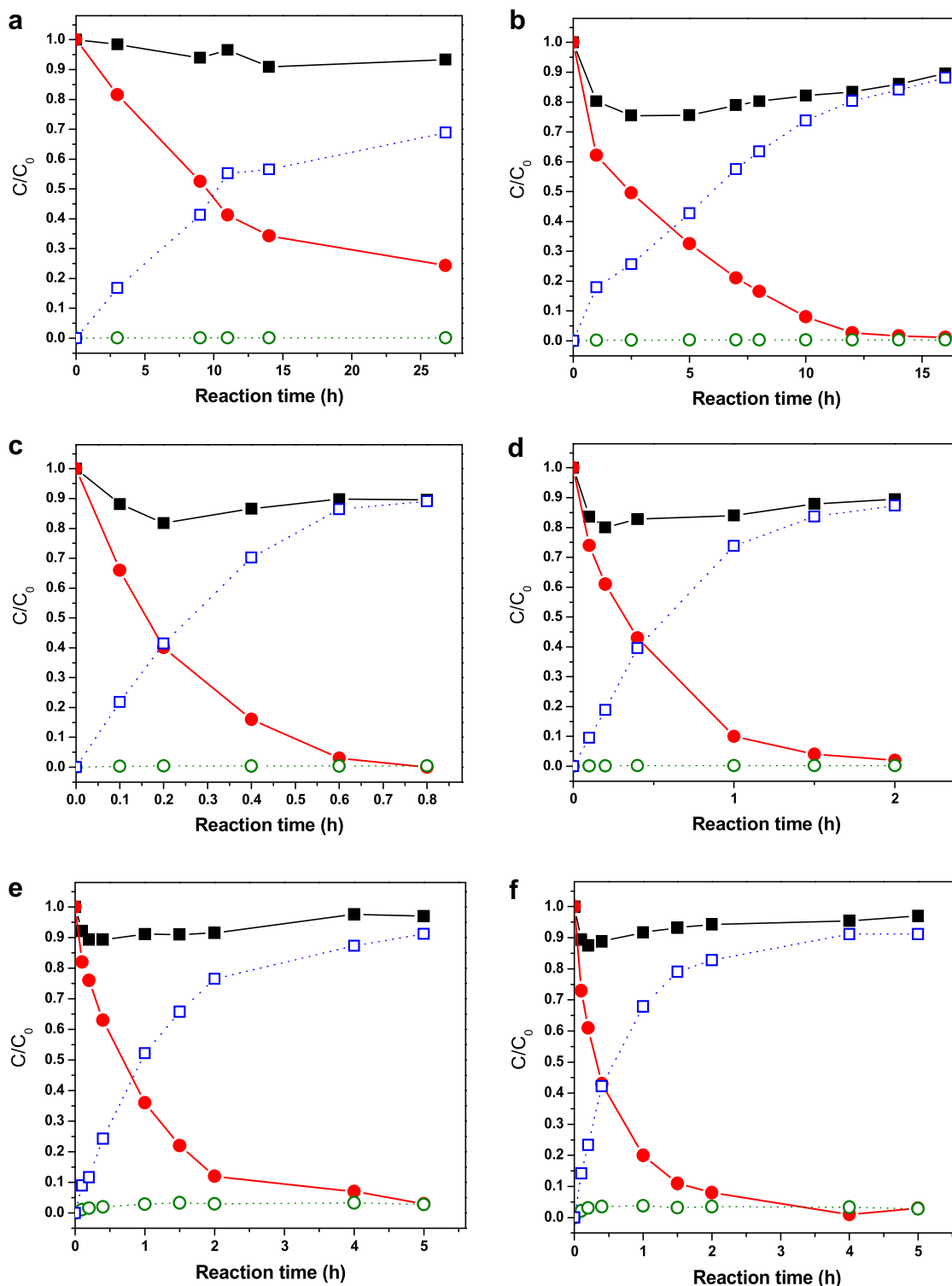**Fig. 3.** Reduction of TCE as function of time by (a) powdered Sn, (b) nano-Sn^0/resin, (c) nano-Pd/Sn/resin, (d) nano-Pd/Sn/resin in 3 mg L^{-1} DO, (e) nano-Pd/Sn/resin in 25 mg L^{-1} NO_3^-, and (f) nano-Pd/Sn/resin in 25 mg L^{-1} HS^-. ■: mass balance, ●: TCE, □: hydrocarbons, and ○: intermediate DECs.

concentration of the hydrocarbon product was estimated with the following equation:

$$[\text{Hydrocarbons}] = \frac{[\text{Excess-free-Cl}^-]}{3} \qquad (9)$$

where the number of 3 is the molar ratio in the Eq. (3). In the powdered Sn system, the carbon mass balance was approximately 91–98% of initial TCE mass. However, a 75–90% recovery efficiency of carbon mass was achieved for both nano-Sn/resin and nano-Pd/Sn/resin. The difference in the recovery efficiencies of carbon mass results from a significant sorption effect exerted by the resin. Because the loss of TCE mass in this closed system was caused by both the degradation by reductive metal (e.g. Sn and Pd/Sn) and sorption into the resin, the estimation of k_{obs} using the sum of k_1 and k_2 was needed. Although DCE isomers were also sorbed into the resin, trace amounts of DCE isomers (below 0.5% of the initial TCE mass) were detected in the powdered Sn, nano-Sn/resin, and nano-Pd/Sn/resin sysytems, indicating that the reaction pathway by β-elimination (Eq. (3)) dominates the reduction of TCE by Sn and Pd/Sn and most of the TCE remains sorbed to the metal surface until complete dechlorination is achieved. Thus, values of k_{obs} would be close to the values of k_1. In this study, the degradation rate of TCE was assumed to be equal to the generation rate of hydrocarbons which were estimated by the generation rate of [Excess-free-Cl$^-$] for eliminating the sorption effect of organic products. Powdered Sn (0.04 mm), nano-Sn/resin (11.8 mg-Sn g^{-1} resin) and nano-Pd/Sn/resin were separately added in the 7 mg L^{-1} TCE solution of 15 mL reactor without headspace. Fig. 3c presents TCE degradation by three reductive materials (powdered Sn, nano-Sn/resin and nano-Pd/Sn/resin) and the related values are shown in Table 1. Regarding the reactivity per unit surface area, the k_{obs} must normalize according to the surface area and the mass concentration of metal particles. The surface area normalized rate constant (k_{SA}) can be calculated by Eq. (10).

$$k_{SA} = \frac{k_{obs}}{\rho_a} \qquad (10)$$

where ρ_a is the surface area concentration of Sn in m^2 L^{-1}. The value of k_{SA} indicates that nano-Sn/resin was 4.5 times more reactive than powdered Sn. After depositing 1% Pd onto nano-Sn/resin, k_{SA} was further enhanced by a factor of 64. In other words, we fabricated a reactive material of nano-Pd/Sn/resin more effective in TCE reduction than commercial powdered Sn, as well as bimetallic particles (e.g. Ni/Fe and Pd/Fe) (Xu et al., 2005).

3.3. Effect of groundwater constituents

Experiments to assess the effects of groundwater containing 3 mg L^{-1} dissolved oxygen (DO), and, 25 mg L^{-1} NO$_3^-$ and 10 mg L^{-1} HS$^-$ on the degradation rates of TCE by nano-Pd/Sn/resin were conducted at pH 7 buffered with 40 mM HEPES. Table 1

shows the values of k_{obs} namely 2.02 ± 0.14, 1.56 ± 0.06 and 1.41 ± 0.07 h^{-1} for groundwater containing DO, NO$_3^-$ and HS$^-$, respectively. The results indicate that DO slightly decreases the k_{obs} value while HS$^-$ and NO$_3^-$ significantly reduces k_{obs} value. Additionally, the concentrations of intermediate DCEs significantly decreased as compared to that in the DI system.

In reactions with bimetallic particles, a relative potential difference drives the electron from the base metal to the second metal, before adsorbed hydrogen ions accept electrons and are converted into adsorbed atomic hydrogen (H$_{ads}$) (Liou et al., 2005). H$_{ads}$, which acts as a reducing agent, has been found to reduce simultaneously various organohalides more quickly than direct electron transfer in monometallic systems (Lin et al., 2004). If H$_{ads}$ existed sufficiently on the noble metal surface, TCE might encounter H-atom donors, forming hydrogenolysis products, e.g. DCEs (Totten et al., 2001). In this system, Pd is believed to catalyze the rapid reaction of O$_2$ and H$_2$ to form water (Eq. (11)) (Fogelberg and Petersson, 1996):

$$2H_2 + O_2 \xrightarrow{\text{Pd}} 2H_2O \qquad (11)$$

The H$_{ads}$ recombination reaction, resulting in the release of hydrogen gas from the second metal surface, is enhanced in the presence of DO. Pd also catalyzes the transformation of NO$_3^-$ to ammonia or N$_2$ in the presence of dissolved H$_2$ (Daub et al., 1999). In this study, near complete transformation of initial NO$_3^-$ to ammonia in the nano-Pd/Sn/resin system was observed. The presence of O$_2$ and NO$_3^-$ affects the Pd ability to transform TCE by competing for H$_{ads}$ on Pd surface. This ultimately leads to a lower TCE transformation rate and DCE production. Addition of 10 mg L^{-1} HS$^-$ resulted in a significant decrease in reaction rates. HS$^-$ appears to be a strong Pd catalyst poison, resulting in rapid Pd catalyst deactivation. This chemisorption to active sites cannot be restored via physical treatments. The groundwater constituents not only dictate reactivity, they also influence selectivity.

3.4. Effect of regeneration

Loss of reactivity of bimetal over time, due to a build up of corrosion products or other precipitates on its surface or the chemisorption of sulfide to the active sites on Pd, is a great concern. The removal of passive oxide layer using acid washing and sonication to restore the reactivity of bimetal has been reported (Lowry
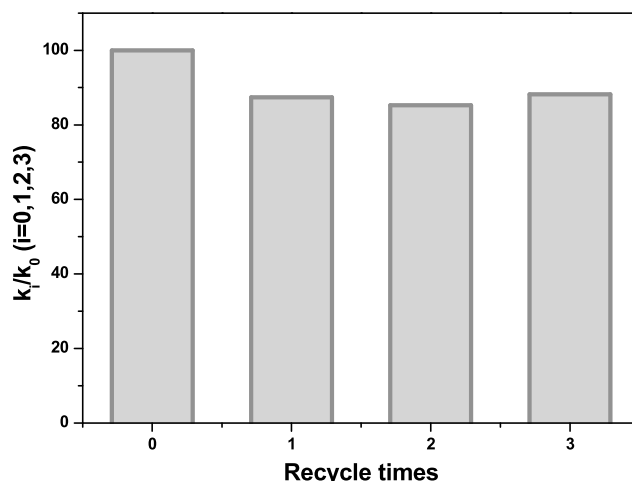
Table 1
The BET surface area and kinetic data of various reductants

Reductants	Specific area (m^2 g^{-1}) (BET)	k_{obs} (h^{-1})	k_{SA} (L h^{-1} m^{-2})
Powdered Sn	0.168	0.09	0.02
Resin	0.040		
Nano-Sn/resin	0.104	0.16 ± 0.01	0.09 ± 0.01
Nano-Pd/Sn/resin	5.9	2.62 ± 0.16	1.22 ± 0.07
[a]Nano-Pd/Sn/resin, O$_2$		2.02 ± 0.14	
[a]Nano-Pd/Sn/resin, NO$_3^-$		1.56 ± 0.06	
[a]Nano-Pd/Sn/resin, HS$^-$		1.41 ± 0.07	

[a] The solutions contain 3 mg L^{-1} dissolved oxygen, and, 25 mg L^{-1} nitrate and 10 mg L^{-1} sulfide, respectively.

Fig. 4. The recovery of reactivity of nano-Pd/Sn/resin immersed in a solution of 10 mg L^{-1} HS$^-$ for 2 d.

and Reinhard, 2001). However, the poisoned sites on Pd surface should be able to be restored though chemical processes. In this study, a 10 wt% NaBH$_4$ solution was used to recover the reactivity of nano-Pd/Sn/resin, by immersion in 10 mg L^{-1} HS$^-$ for 2 d. This regeneration process was similar to the preparation method elucidated above. The rates of TCE reduction in the DI system using the regenerated nano-Pd/Sn/resin were slightly lower than the initial value, indicating that the reactivity of nano-Pd/Sn/resin may not be 100% recoverable (Fig. 4). Presumably, the loosely structured oxides were converted into dense zero valence sites that impeded the exposure of Pd to the solution, and resulted in a loss of the reactivity.

4. Conclusions

We describe a simple preparation method to obtain Pd/Sn bimetallic nanoparticles supported on a cation resin (nano-Pd/Sn/resin) for reductive transformation of aqueous TCE. As compared to commercial powdered Sn, a significant enhancement by ∼2 orders of magnitude in the dechlorination rate was obtained in the nano-Pd/Sn/resin system. Nano-Pd/Sn/resin was successfully synthesized to enhance the removal of TCE from contaminated water. Groundwater constituents such as DO, nitrate and sulfide had significant negative effects on the rate of TCE degradation by nano-Pd/Sn/resin. The regeneration process using a wet-chemical method effectively restored the reactivity of poisoned nano-Pd/Sn/resin with continual dipping in sulfide solution for 2 d. The intermediately chlorinated byproducts at maximum accounted for less than 0.5% of the degraded TCE. These results indicate that nano-Pd/Sn/resin performed well in transforming TCE into nontoxic hydrocarbons, in comparison with other methods.

References

Alessi, D.S., Li, Z., 2001. Synergistic effect of cationic surfactants on perchloroethylene degradation by zero-valent iron. Environ. Sci. Technol. 35, 3713–3717.

Boronina, T., Klabunde, K.J., 1995. Destruction of organohalides in water using metal particles: carbon tetrachloride/water reactions with magnesium, tin, and zinc. Environ. Sci. Technol. 29, 1511–1517.

Chen, J.L., Al-Abed, S.R., Ryan, J.A., Li, Z., 2001. Effects of pH on dechlorination of trichloroethylene by zero-valent iron. J. Hazard. Mater. B83, 243–254.

Cheng, S.F., Wu, S.C., 2000. The enhancement methods for the degradation of TCE by zero-valent metals. Chemosphere 41, 1263–1270.

Choe, S., Chang, Y.Y., Hwang, K.Y., Khim, J., 2000. Kinetic of reductive denitrification by nanoscale zero-valent iron. Chemosphere 41, 1307–1311.

Daub, K., Eming, G., Chollier, M.-J., Callant, M., Dittmeyer, R., 1999. Studies on the use of catalytic membranes for reduction of nitrate in drinking water. Chem. Eng. Sci. 54, 1577–1582.

Doong, R.A., Chen, K.T., Tsai, H.C., 2003. Reductive dechlorination of carbon tetrachloride and tetrachloroethylene by zerovalent silicon–iron reductants. Environ. Sci. Technol. 37, 2575–2581.

Drijvers, D., van Langenhove, H., Kim, L.N.T., Bray, L., 1999. Sonolysis of an aqueous mixture of trichloroethylene and chlorobenzene. Ultroson. Sonochem. 6, 115–121.

Feng, J., Lim, T., 2005. Pathways and kinetics of carbon tetrachloride and chloroform reductions by nano-scale Fe and Fe/Ni particles. Chemosphere 59, 1267–1277.

Fogelberg, J., Petersson, L.G., 1996. Kinetic modelling of the H[2]–O[2] reaction on Pd and of its influence on the hydrogen response of a hydrogen sensitive Pd metal-oxide-semiconductor device. Surf. Sci. 350, 91–102.

Gillham, R.W., O'Hannesin, S.F., 1994. Enhanced degradation of halogenated aliphatics by zero-valent iron. Ground Water 32, 958–967.

Grittini, C., Malcomson, M., Fernando, Q., Korte, N., 1995. Rapid dechlorination of polychlorinated biphenyls on the surface of a Pd/Fe bimetallic system. Environ. Sci. Technol. 29, 2898–2900.

Hung, H.M., Hoffmann, M.R., 1998. Kinetics and mechanism of the enhanced reductive degradation of CCl$_4$ by elemental iron in the presence of ultrasound. Environ. Sci. Technol. 32, 3011–3016.

Kim, Y.H., Carraway, E.R., 2000. Dechlorination of pentachlorophenol by zero valent iron and modified zero valent irons. Environ. Sci. Technol. 34, 2014–2017.

Li, Z., Jones, H.K., Zhang, P., Bowman, R.S., 1999. Enhanced reduction of chromate and PCE by pelletized surfactant-modified zeolite/zerovalent iron. Environ. Sci. Technol. 33, 4326–4330.

Li, Z., Jones, H.K., Zhang, P., Bowman, R.S., 2007. Chromate transport through columns packed with surfactant-modified zeolite/zero valent iron pellets. Chemosphere 68, 1861–1866.

Lin, C.J., Lo, S.L., Liou, Y.H., 2004. Dechlorination of trichloroethylene in aqueous solution by noble metal-modified iron. J. Hazard. Mater. 116, 219–228.

Liou, Y.H., Lo, S.L., Lin, C.J., 2007. Size effect in reactivity of copper nanoparticles to carbon tetrachloride degradation. Water Res. 41, 1705–1712.

Liou, Y.H., Lo, S.L., Lin, C.J., Hu, C.Y., Kuan, W.H., Weng, S.C., 2005. Methods for accelerating nitrate reduction using zero valent iron at near neutral pH: effect of H$_2$-reducing pretreatment and copper deposition. Environ. Sci. Technol. 39, 9643–9648.

Lowry, G.V., Reinhard, M., 2000. Pd-catalyzed TCE dechlorination in groundwater: solute effects, biological control, and oxidative catalyst regeneration. Environ. Sci. Technol. 34, 3217–3223.

Lowry, G.V., Reinhard, M., 2001. Pd-catalyzed TCE dechlorination in water: effect of [H$_2$](aq) and H$_2$-utilizing competitive solutes on the TCE dechlorination rate and product distribution. Environ. Sci. Technol. 35, 696–702.

McCutcheon, S.C., Schnoor, J.L., 2003. Phytoremediation: transformation and control of contaminants. Wiley, New York. pp. 1–10.

Meyer, D.E., Wood, K., Bachas, L.G., Bhattacharyya, D., 2004. Degradation of chlorinated organics by membrane-immobilized nanosized metals. Environ. Prog. 23, 232–242.

Moulder, J.F., Stickle, W.F., Sobol, P.E., Bomben, K.D., 1995. Handbook of X-ray photoelectron spectroscopy. Perkin–Elmer Corporation Physical Electronics, Inc., Minnesota.

Muftikian, R., Fernando, Q., Korte, N., 1995. A method for rapid dechlorination of low molecular weight chlorinated hydrocarbons in water. Water Res. 29, 2434–2439.

Qin, J., Zhang, Q., Chuang, K.T., 2001. Catalytic wet oxidation of p-chlorophenol over supported noble metal catalysts. Appl. Catal. B-Environ. 29, 115–123.

Renolds, G.W., Hoff, J.T., Gillham, R.W., 1990. Sampling bias caused by materials used to monitor halocarbons in groundwater. Environ. Sci. Technol. 24, 135–142.

Roberts, A.L., Totten, L.A., Arnold, W.A., Burris, D.R., Campbell, T.J., 1996. Reductive elimination of chlorinated ethylenes by zero-valent metals. Environ. Sci. Technol. 30, 2654–2659.

Su, C., Puls, R.W., 1999. Kinetics of trichloroethene reduction by zerovalent iron and tin: pretreatment effect, apparent activation energy, and intermediate products. Environ. Sci. Technol. 33, 163–168.

Su, C., Puls, R.W., 2004. Nitrate reduction by zerovalent iron: effects of formate, oxalate, citrate, chloride, sulfate, borate, and phosphate. Environ. Sci. Technol. 38, 2715–2720.

Totten, L.A., Jan, U., Roberts, A.L., 2001. Alkyl bromides as mechanistic probes of reductive dehalogenation: reactions of vicinal dibromide stereoisomers with zerovalent metals. Environ. Sci. Technol. 35, 2268–2274.

Wang, C.B., Zhang, W.X., 1997. Synthesizing nanoscale iron particles for rapid and complete dechlorination of TCE and PCBs. Environ. Sci. Technol. 31, 2154–2156.

Xu, J., Dozier, A., Bhattacharyya, D., 2005. Synthesis of nanoscale bimetallic particles in polyelectrolyte membrane matrix for reductive transformation of halogenated organic compounds. J. Nanopart. Res. 7, 449–467.

Yamazaki, S., Matsunaga, S., Hori, K., 2001. Photocatalytic degradation of trichloroethylene in water using TiO$_2$ pellets. Water Res. 35, 1022–1028.